



^{35}Cl NMR relaxation study of cement hydrate suspensions

Ping Yu^{a,b,*}, R. James Kirkpatrick^{a,c}

^aCenter for Advanced Cement-Based Materials, University of Illinois at Urbana-Champaign, Urbana, IL 61801, USA

^bDepartment of Materials Science and Engineering, University of Illinois at Urbana-Champaign, Urbana, IL 61801, USA

^cDepartment of Geology, University of Illinois at Urbana-Champaign, Urbana, IL 61801, USA

Received 8 January 2001; accepted 25 June 2001

Abstract

^{35}Cl nuclear magnetic resonance (NMR) T_1 and T_2 relaxation study of suspensions of the cement hydrate phases portlandite, $\text{C}_4\text{A}\bar{\text{C}}\text{H}_{11}$ (an AFm phase), and jennite provides significant insight into the mechanisms of chloride sorption in Portland cement systems. For these three phases, all observed chloride is in rapid exchange ($\nu_{\text{ex}} > 1.6$ kHz) between surface and bulk solution sites and is predominantly in a hydrated, solution-like chemical environment. A two-site exchange model for the T_1 relaxation rate data yields sorption densities in excellent quantitative agreement with sorption isotherm measurements for portlandite and $\text{C}_4\text{A}\bar{\text{C}}\text{H}_{11}$. For jennite, the NMR results underestimate the sorption isotherm results by about 40%, but the sorption densities are low, and the results are probably in agreement within experimental error. The observed sorption densities are much greater than can be accommodated by bonding directly to atoms on the solid surfaces and the amount predicted to be in the Stern and diffuse layers by a Gouy-Chapman calculation assuming sorption of only isolated chloride ions. The significance of understanding the structural and dynamical properties of solution-state chloride and the roles of ion pairs and clusters in the solution near the solid surface are discussed. © 2001 Elsevier Science Ltd. All rights reserved.

Keywords: Chloride binding; NMR relaxation rate; Portlandite; AFm; Jennite

1. Introduction

Chloride binding in cement paste and concrete has been widely investigated by pore solution expression, leaching experiments, sorption isotherm measurements, and direct EDAX analyses [1–11]. These methods require drying or separation of the solids from the pore solution, both of which modify the physical and chemical environment at or near the solid/solution interface. It is thus unclear to what extent these results represent the true chloride binding capacity of the samples examined. Binding isotherm studies directly probe the fraction of exchanged and adsorbed chloride in equilibrium with bulk solution [10,12,13], but they provide ambiguous information about the chemical state of the bound species. This paper describes in situ nuclear magnetic resonance (NMR) experiments using solid/solution suspensions that significantly extend the binding capacity results described in Ref. [13] and provide

important new structural and dynamical insight into the binding of chloride ion to cement hydrate phases. A specific objective is to determine whether the binding observed by NMR is the same as observed by sorption isotherm studies. The samples investigated are portlandite ($\text{Ca}(\text{OH})_2$), the AFm carboaluminate hydrate $\text{C}_4\text{A}\bar{\text{C}}\text{H}_{11}$, and jennite. These phases represent model compounds for three important classes of cement paste phases [calcium hydroxide, layer-structured calcium aluminate hydrates, and calcium silicate hydrates (C-S-H)].

Small solute species, such as chloride ion, are in rapid, isotropic, molecular-scale motion, and the experiments described here effectively probe the effects of the solid phase on the motional dynamics. They provide quantitative information about the extent of chloride binding and unique information about exchange rates between bound states at the solid surface and bulk solution. Because these parameters depend on the structure and composition of the solid surface, the data provide useful insight into the nature of these surfaces. To our knowledge, this is the first such microdynamic study of chloride at the surfaces of cement hydrates and indeed one of the few such NMR studies of any solid–aqueous solution system [14].

* Corresponding author. Department of Land, Air and Water Resources, University of California, Davis, CA 95616, USA. Tel.: +1-530-752-2878; fax: +1-630-752-1552.

E-mail address: pyu@ucdavis.edu (P. Yu).

Important NMR parameters used here include the isotropic chemical shift (δ_i), the longitudinal relaxation time (T_1), and the transverse relaxation time (T_2). The chemical shift reflects the local structural (bonding) environment and is related to the electron distribution in and near the observed nucleus [15–17]. T_1 relaxation involves energy exchange between the nuclear spin states and the external environment (the so-called lattice) and is also called spin-lattice relaxation [15–17]. T_1 relaxation must be stimulated and is induced by fluctuation of the magnetic field or electrical field gradient (EFG) at a nucleus (EFG for quadrupolar nuclei only) at the Larmor (resonance) frequency, here 49.005 MHz. For nuclei with spin $I > 1/2$, T_1 relaxation by interaction of the nuclear quadrupole moment and the EFG is normally dominant [18,19]. T_2 relaxation involves dephasing of the precessing nuclear spins by exchange of spin energy among the nuclei in the system but does not result in a change in total spin energy. ^{35}Cl has nuclear spin $I = 3/2$ and a quadrupole moment of $-7.89 \times 10^{-28} \text{ m}^2$, and its relaxation is dominated by quadrupole effects. The rate of chloride quadrupolar relaxation in aqueous systems is sensitive to the chloride and counter-ion concentrations [20]. Here, comparison of chloride relaxation in neat solutions and in suspensions of cement hydrate phases provides important information about chloride binding at the solid surface.

2. Experimental

2.1. Cement hydrate suspensions

The cement hydrate phases were prepared as described in Ref. [13] and were mixed with lime-saturated NaCl solutions for the NMR experiments. The sodium chloride concentrations ranged from 0.001 to 4 M ($M = \text{mol/L}$), and the solutions were made by dissolving reagent-grade NaCl (Fisher Scientific, Fair Lawn, NJ, USA) in saturated lime water. The suspensions were made by adding weighed amounts of the desired NaCl solution to the solid powder in a glass NMR tube 5 mm in diameter and 1.5 cm in length. The solid/solution ratio was controlled to maintain a homogeneous suspension and was kept constant for each solid phase such that the chloride concentration is the only variable. The solid/solution ratios (g/g) for the suspensions of portlandite, $\text{C}_4\text{A}\bar{\text{C}}\text{H}_{11}$, and jennite were 0.70, 0.40, and 0.15, respectively.

2.2. ^{35}Cl NMR relaxation experiments

Static ^{35}Cl NMR experiments were performed using a home-built pulse-Fourier transform NMR spectrometer based on an 11.7 T superconducting solenoid magnet (Oxford Instrument, UK) and a MacNMR-5.3 data acquisition/processing system (TECMAG, Houston, TX, USA). The probe was home built. T_1 and T_2 relaxation data for the

suspensions were collected at a Larmor frequency (ω_0) of 49.005 MHz using a $\pi/2$ pulse width of 8 μs and from 4 to 400 transients, depending on the chloride concentration. ^{35}Cl NMR chemical shifts were externally referenced to 1 M NaCl solution. T_1 relaxation rates were measured for the suspensions and initial NaCl solutions using an inversion-recovery sequence [21,22] with 13 spectra and τ values of 1–200 ms. A stretched exponential decay function ($M_t/M_0 = 1 - 2 \exp[-(t/T_1)^\beta]$) was used to fit the data for T_1 calculation. T_2 relaxation rates were measured using a Carr-Purcell-Meiboom-Gill pulse sequence [21,22] with 15 spectra and τ values of 1–100 ms. A simple exponential decay $M_t/M_0 = \exp(-t/T_2)$ was adequate to fit the data. The delay time for all the relaxation measurements was 200 ms. All experiments were conducted at 20°C.

3. Results and interpretation

3.1. ^{35}Cl NMR spectra of hydrate suspensions

The static ^{35}Cl NMR spectra of the suspensions of portlandite, $\text{C}_4\text{A}\bar{\text{C}}\text{H}_{11}$, and jennite at 20 °C exhibit only one narrow peak near 0 ppm (Fig. 1). For the portlandite and $\text{C}_4\text{A}\bar{\text{C}}\text{H}_{11}$ suspensions, the observed peak width decreases with increasing chloride concentration, whereas for the jennite suspensions, it does not change significantly. The absence of separately resolvable signal for surface-bound chloride demonstrates that the observed chloride is in rapid exchange with the bulk solution at a frequency $> \sim 1.6 \text{ kHz}$ ($10 \times$ the peak width at half-height) and is thus not tightly bound to the solid surface [23,24]. The presence of only one

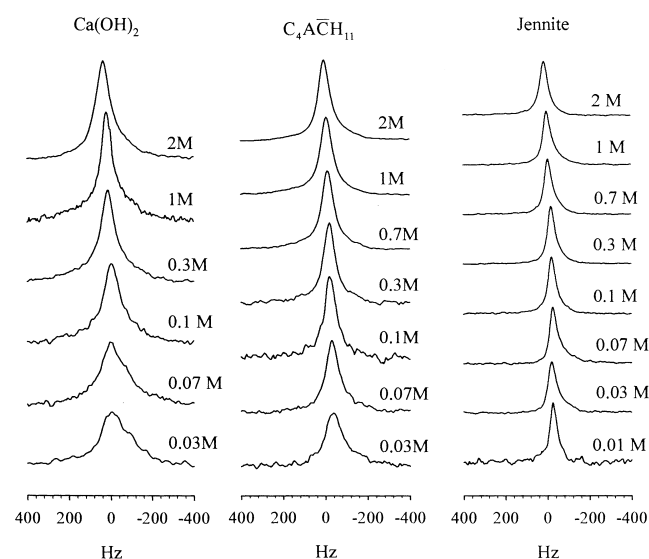


Fig. 1. Static ^{35}Cl NMR spectra of suspensions of the indicated solid phase in Ca hydroxide-saturated NaCl solutions with the indicated concentrations. Variation of the full width at half-height is related to the effects of the surface on the rate of T_2 relaxation; see text for an explanation.

peak allows analysis of the signals using classical NMR theory for systems undergoing so-called rapid exchange. The chemical shift near 0 ppm indicates a predominantly solvated nearest-neighbor structural environment comparable to that in solution.

For neat solutions, the NMR peak width is related to the T_2 relaxation rate via $1/T_2 = \pi\nu_{1/2}$, where $\nu_{1/2}$ is the full width at half-height (FWHH) of the NMR signal [25]. The observed decrease in peak width with increasing chloride concentration thus indicates a decreasing average T_2 relaxation rate for Cl^- in the suspensions. This trend is opposite the known variation for chloride T_2 values in neat solutions, as shown by the data in Fig. 2 and in the literature [20]. Thus, qualitatively, the changing peak widths for the portlandite and AFm suspensions indicate larger T_2 values for chloride on the surface and significantly greater interaction of these phases with solution chloride than for jennite. The following direct measurements of the relaxation rates of the suspensions provide a more quantitative view.

3.2. ^{35}Cl NMR relaxation of the hydrate suspensions

For a given hydrate phase, the measured T_1 and T_2 relaxation rates of all the suspensions are identical within experimental error, as expected in the extreme narrowing limit [18,19]. Here, we use the T_1 relaxation rates, because they are more precisely measured experimentally. The observed T_1 relaxation behavior is essentially single-exponential. The stretching parameter, β , averages about 0.96 and does not vary systematically with solid/solution ratio. The measured T_1 relaxation rates ($R_1 = 1/T_1$) of the suspensions vary significantly with bulk chloride concentration

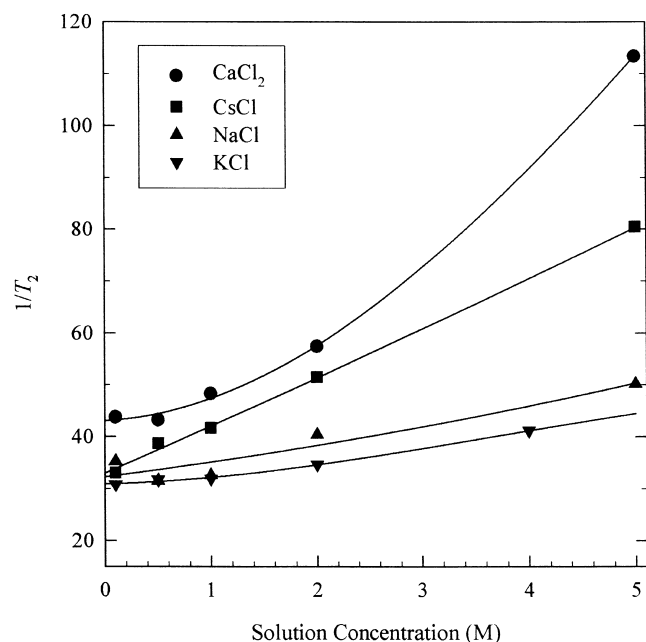


Fig. 2. ^{35}Cl NMR T_2 relaxation rates of chloride salt solutions as a function of Cl^- concentration.

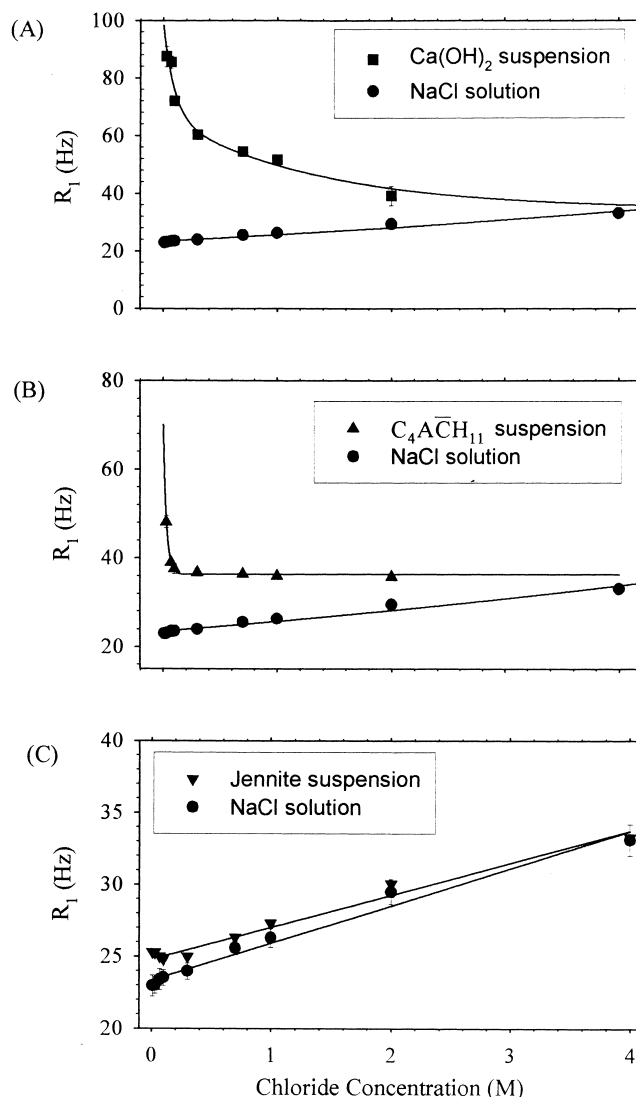


Fig. 3. ^{35}Cl NMR T_1 relaxation rates of suspensions of cement hydrate phases in NaCl solutions plotted vs. solution chloride concentration.

and approach the values of the neat solutions at high concentrations (Fig. 3). For the portlandite suspensions, R_1 decreases with increasing concentration at all observed values. For the $\text{C}_4\text{A}\bar{\text{C}}\text{H}_{11}$ suspensions, R_1 decreases rapidly at low concentrations and remains nearly constant at higher concentrations. For the jennite suspensions, R_1 decreases slightly at low concentration and then increases at higher concentrations. For all the phases, these results clearly indicate that the fraction of the surface-bound chloride decreases with increasing bulk chloride content, consistent with the sorption isotherm data for them (Freunlich-type isotherms) [13] and the ^{35}Cl peak widths (Fig. 1). The NMR relaxation rates for the surface-bound species are well known to be greater than for the same species in bulk solution [14,18,19]. This is because the correlation times of rotational motion of water molecules coordinated to small ions in aqueous solutions are greater than the NMR reso-

nance frequencies, and surface binding decreases these correlation times, thus increasing the intensity of the power spectrum at the resonance frequency.

The magnitude of the difference of the T_1 relaxation rates of a suspension and the neat solution with the same composition reflects the affinity of the surface for chloride. Thus, the data in Fig. 3 indicate a decreasing chloride affinity from portlandite to $C_4A\bar{C}H_{11}$ to jennite. The observation that the T_1 relaxation rates of jennite suspensions are only slightly higher than those of the neat solutions indicates that only a small fraction of the chloride is sorbed for this sample, in agreement with the sorption isotherm, linewidth, and T_2 data.

4. Discussion

4.1. Chloride binding capacity

Under conditions of rapid exchange between two chemical environments, it is sometimes possible to use the observed relaxation rates to determine the relative fractions of the two sites [14,26], and this method provides excellent fits to the data here. In this two-site exchange model,

$$R_{\text{obs}} = (1-\alpha)R_F + \alpha R_B \quad (1)$$

where R_{obs} , R_F , and R_B are the T_1 or T_2 (here, $T_1 = T_2$) relaxation rates of the net suspension, neat solution, and sorbed species, and α is the fraction of sorbed species (here chloride). R_{obs} and R_F are experimentally measured, and R_B can be determined by extrapolation to extreme dilution (when $\alpha \rightarrow 1$). The estimated R_B values are 98.4 Hz for portlandite (about four times of that of the neat solution, 23.3 Hz), 70.0 Hz for AFm (about three times of that of the neat solution), and 25.5 Hz for jennite (only slightly larger than that of the neat solution). The R_B values are best thought of as average values for all the surface chlorides. Because there are multiple possible surface sites and R_B probably varies with concentration in the Stern and diffuse layers, individual chloride nuclei will certainly have a range of instantaneous R_B values. Because signal is entirely averaged, however, only the average value can be determined.

Assuming that R_B does not change with bulk solution chloride concentration and that R_F is the same as for the neat solution, Eq. (1) allows direct calculation of the concentration dependence of the relative abundance of the bound and solution state chloride for all the samples (Fig. 4). As expected qualitatively from the peak widths, the fraction of bound chloride decreases with increasing solution concentration for all three phases. This is consistent with the sorption isotherm studies [13] and confirms the qualitative interpretations above that the affinity for chloride decreases from portlandite to $C_4A\bar{C}H_{11}$ to jennite.

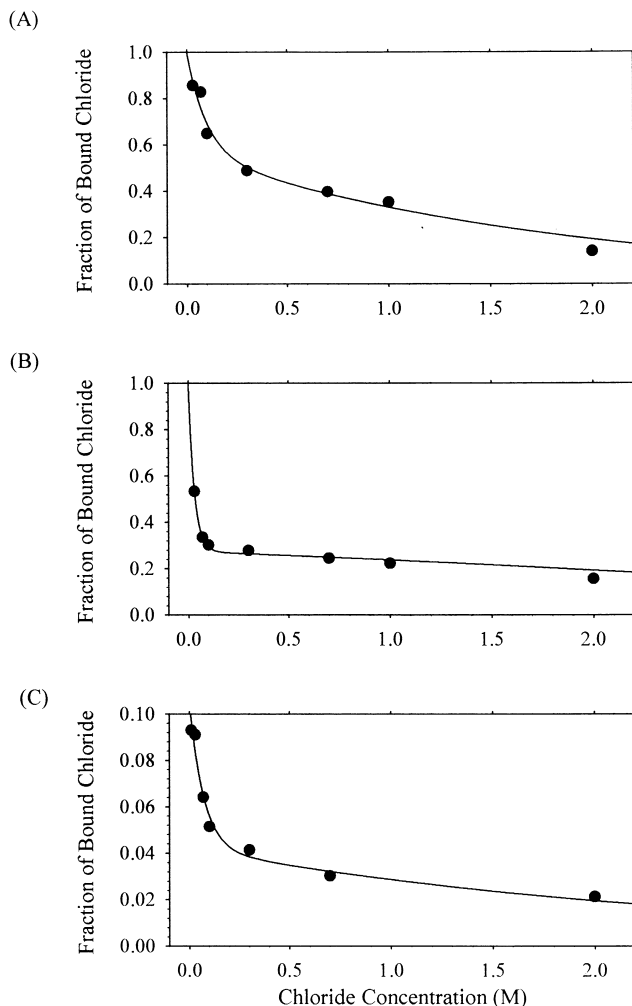


Fig. 4. Fraction of sorbed chloride (left vertical axis) and sorption density of cement hydrate phases (right vertical axis) plotted vs. initial chloride concentration (bottom horizontal axis) and total chloride/surface area ratio (top horizontal axis): (A) $\text{Ca}(\text{OH})_2$; (B) $C_4A\bar{C}H_{11}$; (C) jennite.

Although the fraction of bound chloride decreases with increasing solution concentration, the surface area-normalized binding density (the number density of bound chloride atom per square nanometer of solid surface) increases with a relationship that is concave to the concentration axis without reaching a plateau (Fig. 5). Indeed, the values for portlandite and AFm are in excellent quantitative agreement with the values determined from the sorption isotherm measurements described in Ref. [13] (Fig. 5). For the jennite, the values determined from the NMR data are about 40% less than those from the sorption isotherm data, but the total sorption densities are low, and the differences of about $2\text{--}4 \text{ Cl}^-/\text{nm}^2$ are probably within analytical error.

The high affinities of portlandite and AFm for chloride cannot be adequately understood by reference to just their surface structures. The portlandite structure consists of neutral $\text{Ca}(\text{OH})_6$ octahedral sheets, and the density of hydroxyl groups on the basal plane is $8.94 \text{ OH}/\text{nm}^2$. This is the largest possible density of directly bound chloride if each

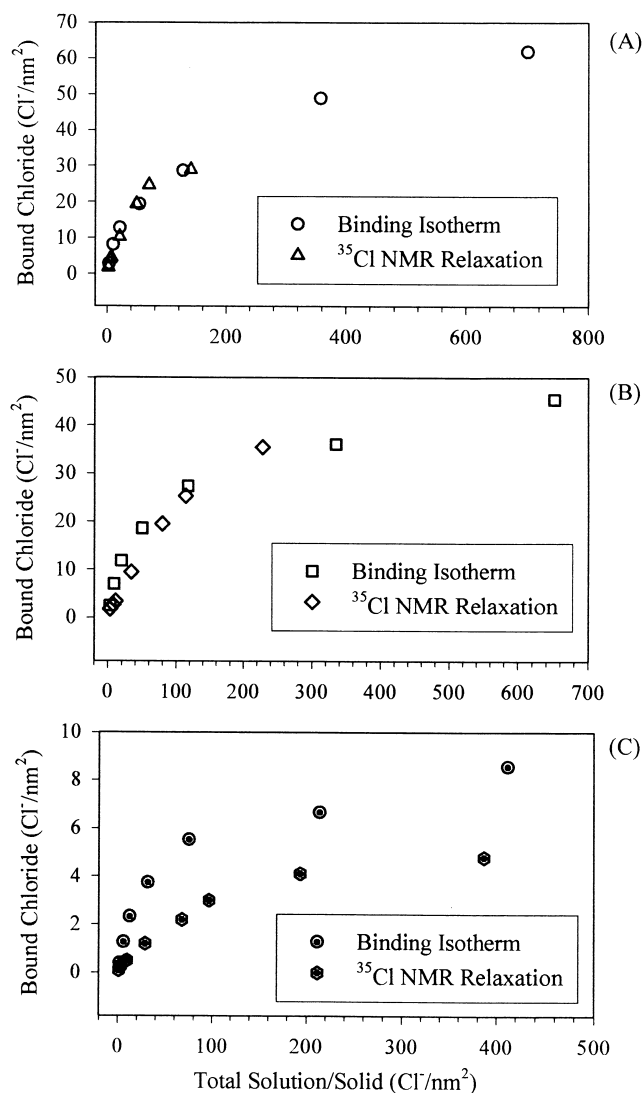


Fig. 5. Comparison of chloride sorption densities determined from the ³⁵Cl NMR *T*₁ relaxation rates and from sorption isotherm data [13] plotted vs. total chloride/solid-surface ratio: (A) portlandite; (B) C₄ĀCH₁₁; (C) jennite.

surface hydroxyl is hydrogen bonded to an average of one chloride. Recent molecular dynamics simulations of chloride binding on portlandite suggests, however, that each chloride is coordinated to three surface OH-groups (A. Kalinichev, personal communication), reducing this density to about $\sim 3 \text{ Cl}^-/\text{nm}^2$. Either of these values is significantly lower than the maximum observed density of $\sim 30 \text{ Cl}^-/\text{nm}^2$. The structures of AFm phases consist of positively charged $[\text{Ca}_2\text{Al}(\text{OH})_6]^+$ layers balanced by interlayer and surface anions together with water molecules [27–33]. The charge density of the (001) surface is $e/(a_0 \cdot b_0) = 1.741 \text{ e}/\text{nm}^2$, based on its crystallographic parameters [27]. This charge density would support a surface chloride density of about this value or perhaps somewhat more if hydrogen bonding were important (as for portlandite). In either case, the amount of directly bound chloride must be substantially less than the maximum value of $36 \text{ Cl}^-/\text{nm}^2$.

These ideas, in conjunction with the similarly low values of the amount of sorbed chloride calculated from the multi-layer models [13], strongly suggest that simple electrostatic or hydrogen bonding attraction of isolated chloride ion to the surface is not the principal mechanism for chloride sorption to these phases. As discussed in Ref. [13], coadsorption of chloride and cations (ion pair or ion cluster formation) could increase the chloride binding capacity. NMR spectroscopy would sample signal from such coadsorbed chloride. In this model, the total sorbed chloride is that needed to balance the positive surface charge of the solid plus the positive charge of a large number of sorbed cations.

C-S-H phases, like clay minerals, carry a negative structural charge on their basal surfaces [34] but may have either positive or negative charges on particle edges, depending on the details of the surface structure and the composition of the solution. The jennite structure, although not fully understood, is thought to be broadly similar to that of tobermorite with every other silicate chains replaced by rows of Ca-OH sites and concomitant rearrangement of the Ca-layer [34]. The abundant surface CaOH groups appear to play a prominent role in chloride sorption.

4.2. Chloride binding environments

Taken together, the ³⁵Cl NMR relaxation rates described here and the sorption isotherm data described in Ref. [13] provide a picture of dominantly nonspecific sorption. Most of the chloride associated with the surfaces of cement hydrate phases varying from portlandite to AFm to Ca-silicates is in a solvated structural environment similar to that in aqueous solution. This chloride is in rapid exchange with the solution at frequencies $>1.6 \text{ kHz}$, and the amount of sorbed chloride is much greater than can be accommodated in a single surface layer. The ³⁵Cl NMR and molecular modeling results for surface chloride on Friedel's salt [35] and the molecular modeling results for chloride on portlandite [36], however, show that at any instant at least some of the chloride associated with these phases is likely to be held as inner sphere complexes. For portlandite, the chemical shift of this inner sphere chloride does not appear to be much different from solution chloride [24], probably because both the surface and water offer OH groups as the nearest neighbors to the chloride ions and because in a suspension the surface chloride retains many of its coordinating water molecules. The diffuse layer can usefully be thought of as a highly concentrated solution, and as described in Ref. [13], a principal question is how the observed binding can be so much larger than expected from Gouy-Chapman theory.

Better understanding the structural and thermodynamic properties of chloride in concentrated, high pH aqueous solutions relevant to cement chemistry is essential to interpretation of the NMR and sorption isotherm results. Currently available data indicate that a significant fraction of the bound chloride occurs in ion clusters containing Ca and Cl near the solid surface. Relevant molecular-scale parameters

for aqueous chloride include the average coordination number, bond length and bond strength to its nearest neighbors, the rate of exchange between its coordinating hydration waters and bulk water, and the concentrations and structures of ion pairs or ion clusters in which it participates. These have been investigated extensively by X-ray and neutron diffraction (XRD and ND) [37,38], X-ray absorption spectroscopy (EXAFS and XANES) [37], NMR (^1H , ^2D , ^{27}O , and ^{35}Cl) [37,39–42], IR and Raman spectroscopy [37], and molecular dynamics computation [43,44]. The following is a summary of the important points from these references.

For Na and Ca chloride solutions, neutron diffraction shows that the average chloride coordination number is 5.5 and 5.8, respectively [37,39]. Neutron diffraction also indicates that each water molecule in the nearest-neighbor hydration sphere forms one hydrogen bond to the chloride ion [45]. The observed rotational correlation times and activation energies of water exchange in the first hydration sphere show that the ion–water bond strength is greater for Ca and Na than for chloride [38]. The rotational frequency of water molecules hydrating chloride is 4×10^{11} Hz [42] and the lifetime of a $\text{Cl}(\text{H}_2\text{O})_6^-$ complex is less than 10 ps [45]. Surface force experiments and dielectric constant measurements suggest that near the surfaces of metal oxides and clay minerals, water has a more ordered structure and is less able to reorient its dipoles due to presence of the electric field of the solid [46]. The stronger hydrogen bonding and more ordered packing of the surface water relative to the water in bulk solution lead to a longer correlation time of reorientation, which increases the density of the power spectrum at the chloride Larmor frequency ($\sim 10^7$ Hz) and enhances quadrupole relaxation. It is reported that surface-adsorbed water has a much lower permittivity, which is favorable to ion-pair formation [46].

It is quite common that in concentrated electrolyte solutions, ion pairs and complexes are formed by sharing water molecules in the first hydration sphere or by ligand exchange [37]. Although the nearest-neighbor coordination shell of chloride is difficult to study due to weak hydration, cation hydration can be readily explored by diffraction and EXAFS methods and provides useful insight into the problems here [37]. Ion cluster formation by substitution of chloride ions for water molecules in the first hydration sphere of cations increases from Na^+ to K^+ to Ca^{2+} to Cs^+ [37]. In hydrated cement paste, Ca^{2+} ions tend to preferentially accumulate at the surface of the solid [47]. The positive surface potential of early hydration product of cement, for instance, is thought to be due to adsorption of Ca^{2+} on the hydrate surface [48].

5. Conclusions

^{35}Cl NMR relaxation methods and a two-site exchange model are shown to be useful tools to study the in situ molecular-scale structural and dynamical properties of

chloride sorbed on cement hydrate phases in contact with aqueous chloride solutions. The results indicate that the majority of the sorbed chloride near the surfaces of solid phases as diverse as portlandite, $\text{C}_4\text{A}\bar{\text{C}}\text{H}_{11}$, and jennite is in a solution-like environment and is in rapid exchange (exchange frequency >1.6 kHz) with free chloride in the bulk solution. The ^{35}Cl NMR T_1 relaxation data indicate that portlandite and $\text{C}_4\text{A}\bar{\text{C}}\text{H}_{11}$ (and by extension other AFm phases) have relatively high chloride binding capacities, whereas that for jennite is relatively low. The surface chloride densities obtained from a two-site exchange model of the ^{35}Cl NMR T_1 relaxation data for portlandite and $\text{C}_4\text{A}\bar{\text{C}}\text{H}_{11}$ are in excellent quantitative agreement with the values obtained in a sorption isotherm study of the same phases [13]. For jennite, the NMR results are about 40% lower than the sorption isotherm results, but the total sorption is low, and the results probably agree within experimental error. The total amount of sorbed chloride is substantially greater than can be accommodated by coordination directly to the solid surfaces and the amount predicted to exist in the Stern and diffuse layers based on a Gouy-Chapman calculation (see Ref. [13]). This excess is probably due primarily to formation of metal (probably Ca^{2+})-Cl complexes or ion pairs.

References

- [1] S. Nagataki, N. Otsuki, T.-H. Wee, K. Nakashita, Condensation of chloride ion in hardened cement matrix materials and on embedded steel bars, *ACI Mater. J.* 90 (4) (1993) 323–332.
- [2] M. Castellote, A. Andrade, C. Alonso, Chloride-binding isotherms in concrete submitted to non-steady-state migration experiments, *Cem. Concr. Res.* 29 (1999) 1799–1806.
- [3] A. Delagrave, J. Marchand, J.-P. Ollivier, S. Julien, K. Hazrati, Chloride binding capacity of various hydrated cement paste systems, *Adv. Cem. Based Mater.* 6 (1997) 28–35.
- [4] S. Diamond, Chloride concentrations in concrete pore solutions resulting from calcium and sodium chloride admixtures, *Cem. Concr. Aggregates* 8 (2) (1986) 97–102.
- [5] O. Franc, R. Francois, Measuring chloride diffusion coefficients from non-steady state diffusion tests, *Cem. Concr. Res.* 28 (7) (1998) 947–953.
- [6] G.K. Glass, G.M. Stevenson, N.R. Buenfeld, Chloride-binding isotherms from the diffusion cell test, *Cem. Concr. Res.* 28 (7) (1998) 939–945.
- [7] M.N. Haque, O.A. Kayyali, Aspect of chloride ion determination in concrete, *ACI Mater. J.* 92 (9/10) (1995) 532–541.
- [8] C.L. Page, Ø. Vennesland, Pore solution composition and chloride binding capacity of silica-fume cement pastes, *Mater. Constr.* 16 (1983) 19–25.
- [9] A.K. Suryavanshi, J.D. Scantlebury, S.B. Lyon, Mechanism of Friedel's salt formation in cements rich in tri-calcium aluminate, *Cem. Concr. Res.* 26 (5) (1996) 717–727.
- [10] L. Tang, L.-O. Nilsson, Chloride binding capacity and binding isotherms of OPC pastes and mortars, *Cem. Concr. Res.* 23 (2) (1993) 247–253.
- [11] U. Wiens, P. Schiessl, Chloride binding of cement paste containing fly ash, in: *Proceedings of the 10th international congress on the chemistry of cement*, Gothenburg, Sweden, June 2–6, 1997, Volume 4 (Performance and durability of cementitious materials) 4iv016, 10 pp.

- [12] J.J. Beaudoin, V.S. Ramachandran, R.F. Feldman, Interaction of chloride and C-S-H, *Cem. Concr. Res.* 20 (1990) 875–883.
- [13] P. Yu, R.J. Kirkpatrick, Chloride binding to cement hydrate phases: Binding isotherm studies. *Cem. Concr. Res.*, submitted for publication.
- [14] Y.K. Kim, R.J. Kirkpatrick, NMR T_1 relaxation study of ^{133}Cs and ^{23}Na adsorbed on illite, *Am. Mineral.* 83 (1998) 661–665.
- [15] R.K. Harris, Nuclear magnetic resonance spectroscopy, a physico-chemical view, Longman, Harlow, 1986.
- [16] C.P. Slichter, Principles of Magnetic Resonance, third ed., Springer-Verlag, Berlin, 1990.
- [17] R. Abraham, J. Fisher, P. Loftus, Introduction to NMR Spectroscopy, Wiley, Chichester, 1988.
- [18] B. Lindman, S. Forsen, Chloride, bromine and iodine NMR, in: P. Diehl, E. Fluck, R. Kosfeld (Eds.), Physico-Chemical and Biological Applications, NMR Basic Principles and Progress, vol. 12, Springer-Verlag, Berlin, 1976, pp. 1–203.
- [19] B. Lindman, S. Forsen, The halogen-chlorine, bromine and iodine, in: R.K. Harris, B.E. Mann (Eds.), NMR and the Periodic Table, Academic Press, New York, 1978, pp. 421–438.
- [20] M. Holz, H. Weingartner, Magnetic relaxation of chloride ions in aqueous solutions, *J. Magn. Reson.* 27 (1977) 153–155.
- [21] H. Güthner, NMR Spectroscopy, Basic Principles, Concepts, and Applications in Chemistry, second ed., Wiley, New York, 1992.
- [22] E. Fukushima, S.B.W. Roeder, Experimental Pulse NMR: A Nuts and Bolts Approach, Addison-Wesley Publishing, Reading, 1981.
- [23] C.A. Weiss, R.J. Kirkpatrick, S.P. Altaner, The structural environments of cations adsorbed onto clays: ^{133}Cs variable-temperature MAS NMR spectroscopy of hectorite, *Geochim. Cosmochim. Acta* 54 (1990) 1655–1669.
- [24] R.J. Kirkpatrick, P. Yu, X. Hou, Y. Kim, Interlayer structure, anion dynamics, and phase transitions in mixed-metal layered hydroxides: Variable temperature ^{35}Cl NMR spectroscopy of hydrotalcite and Ca-aluminate hydrate (hydrocalumite), *Am. Mineral.* 84 (1999) 1186–1190.
- [25] R.K. Harris, B.E. Mann, NMR and the Periodic Table, Academic Press, New York, 1978, pp. 1–19.
- [26] J. Kowalewski, Nuclear spin relaxation in diamagnetic fluids: Part 1. General aspects and inorganic applications, in: G.A. Webb (Ed.), Annual Reports on NMR Spectroscopy, vol. 22, Academic Press, San Diego, 1989, pp. 308–414.
- [27] A. Terzis, S. Filippakis, H.-J. Kuzel, H. Burzlaff, The crystal structure of $\text{Ca}_2\text{Al}(\text{OH})_6\text{Cl}\cdot 2\text{H}_2\text{O}$, *Z. Kristallogr.* 181 (1987) 29–34.
- [28] H.F.W. Taylor, Crystal structure of some double hydroxide minerals, *Mineral. Mag.* 39 (1973) 377–389.
- [29] R. Fischer, H.-J. Kuzel, Reinvestigation of the system $\text{C}_4\text{A}\cdot n\text{H}_2\text{O}\cdot \text{C}_4\text{A}\cdot \text{CO}_2\cdot n\text{H}_2\text{O}$, *Cem. Concr. Res.* 12 (1982) 517–526.
- [30] M. Francois, G. Renaudin, O. Evrard, A cementitious compound with composition $3\text{CaO}\cdot\text{Al}_2\text{O}_3\cdot\text{CaCO}_3\cdot 11\text{H}_2\text{O}$, *Acta Crystallogr. C* 54 (1998) 1214–1247.
- [31] G. Renaudin, M. Francois, O. Evrard, Order and disorder in the lamellar hydrated tetracalcium monocarboaluminate compound, *Cem. Concr. Res.* 29 (1999) 63–69.
- [32] M. Sacerdoti, E. Passaglia, Hydrocalumite from Latium, Italy: Its crystal structure and relationship with related synthetic phases, *N. Jb. Miner. Mh.* 1988 (10) (1988) 462–475.
- [33] E. Passaglia, M. Sacerdoti, Hydrocalumite from Montalto di Castro, Viterbo, Italy, *N. Jb. Miner. Mh.* 1988 (10) (1988) 454–461.
- [34] H.F.W. Taylor, Cement Chemistry, second ed., Thomas Telford, London, 1997.
- [35] A.G. Kalinichev, R.J. Kirkpatrick, R.T. Cygan, Molecular modeling of the structure and dynamics of the interlayer and surface species of mixed-metal layered hydroxides: Chloride and water in hydrocalumite (Friedel's salt), *Am. Mineral.* 85 (2000) 1046–1052.
- [36] A.G. Kalinichev, R.J. Kirkpatrick, Molecular dynamics modeling of chloride binding to the surface of portlandite, hydrated Ca-silicate and Ca-aluminate phases, *Cem. Concr. Res.*, submitted for publication.
- [37] H. Ohtaki, T. Radnai, Structure and dynamics of hydrated ions, *Chem. Rev.* 93 (3) (1993) 1157–1204.
- [38] L. Endom, H.G. Hertz, M.D. Zeidler, A microdynamic model of electrolyte solutions as derived from nuclear magnetic relaxation and self-diffusion data, *Ber. Bunsen-Ges.* 71 (9/10) (1967) 1008–1031.
- [39] J.E. Enderby, S. Cummings, G.J. Herdman, G.W. Neilson P.S. Salmon, N. Skipper, Diffraction and the study of aqua ions, *J. Phys. Chem.* 91 (1987) 5851–5858.
- [40] R.P.W.J. Struis, J. de Bleijser, J.C. Leyte, $^{25}\text{Mg}^{2+}$ and $^{35}\text{Cl}^-$ quadrupolar relaxation in aqueous MgCl_2 solutions at 25°C: 1. Limiting behavior for infinite dilute, *J. Phys. Chem.* 93 (1989) 7932–7942.
- [41] R.P.W.J. Struis, J. de Bleijser, J.C. Leyte, $^{25}\text{Mg}^{2+}$ and $^{35}\text{Cl}^-$ quadrupolar relaxation in aqueous MgCl_2 solutions at 25°C: 2. Relaxation at finite MgCl_2 concentrations, *J. Phys. Chem.* 93 (1989) 7943–7952.
- [42] H.G. Hertz, Magnetic relaxation by quadrupole interaction of ionic nuclei in electrolyte solutions: Part I. Limiting values for infinite dilute, *Ber. Bunsen-Ges.* 77 (7) (1973) 531–540.
- [43] D.G. Bounds, A molecular dynamics study of the structure of water around the ions Li^+ , Na^+ and K^+ , Ca^{++} , Ni^{++} and Cl^- , *Mol. Phys.* 54 (6) (1985) 1335–1355.
- [44] R.W. Impey, P.A. Madden, I.R. McDonald, Hydration and mobility of ions in solution, *J. Phys. Chem.* 87 (1983) 5071–5083.
- [45] J.P. Hunt, H.L. Friedman, Aquo complexes of metal ions, in: S.J. Lippard (Ed.), Progress in Inorganic Chemistry, vol. 30, Wiley, New York, 1983, pp. 359–387 (An Interscience Publication).
- [46] G.E. Brown Jr., V.E. Henrich, W.H. Casey, D.L. Clark, C. Eggleston, A. Felmy, D.W. Goodman, M. Grätzel, G. Maciel, M.I. McCarthy, K.H. Nealson, D.A. Sverjensky, M.F. Toney, J.M. Zachara, Metal oxide surfaces and their interactions with aqueous solutions and microbial organisms, *Chem. Rev.* 99 (1999) 77–174.
- [47] S. Chatterji, M. Kawamura, Electrical double layer, ion transport and reactions in hardened cement paste, *Cem. Concr. Res.* 22 (1992) 774–782.
- [48] V.S. Ramachandran, Possible states of chloride in the hydration of tricalcium silicate in the presence of calcium chloride, *Mater. Constr.* 4 (1971) 3–12.